

# First Results from a Combined Weak-Lensing and X-ray Search for Galaxy Clusters

Jörg Dietrich<sup>1</sup>, Axel Schwobe<sup>2</sup>, Thomas Erben<sup>1</sup>, Peter Schneider<sup>1</sup>, Georg Lamer<sup>2</sup>

<sup>1</sup>IAEF, University of Bonn, Germany, <sup>2</sup>Astrophysikalisches Institut Potsdam, Germany

## Abstract

We present first results from a combined weak lensing, X-ray, and optical search for galaxy clusters with the Wide Field Imager (WFI) at the ESO/MPG-2.2 m telescope and XMM-Newton archival data. Our survey will eventually cover an area of 6 square degrees on deep XMM-Newton serendipitous fields, allowing the immediate comparison of lensing detected cluster candidates to X-ray data. The combination of X-ray, optical, and weak lensing detection of clusters will allow us to study their respective selection functions and understand potential biases.

## 1 Introduction

The population of galaxy clusters evolves with redshift, and this evolution depends on the cosmological model (e.g., Eke et al. 1996). Therefore, the redshift dependence of the cluster abundance has been used as a cosmological test (e.g., Vikhlinin et al. 2003; Henry 2004). The dependence of the cluster abundance on cosmological parameters can be obtained either from analytical models (Press & Schechter 1974), or more reliably from N-body simulations (e.g., Jenkins et al. 2001). What such models predict is the abundance of dark matter halos as a function of redshift and mass.

Clusters can be selected by various methods: optical, X-ray emission, weak lensing, and – using future surveys – the Sunyaev-Zeldovich effect (SZE). SZE, optical, and X-ray selection of clusters depends on the baryonic content of clusters, which – compared to the predicted dark matter density – is a minor fraction of the clusters' constituents. Optical selection depends on the star formation history, and X-ray and SZE detection requires a hot intra-cluster medium (ICM). Weinberg & Kamionkowski (2002) predict that up to 20% of all weak lensing clusters have not heated their ICM to a level detectable with current X-ray missions. Searching for clusters with SZE is a very promising method but has yet to produce first samples. All four selection methods are sensitive in different redshift regimes. Clearly, no cluster selection method is ideal, and understanding their biases and limitations is important for precision cosmology using clusters.

## 2 Survey Overview

We present first results from a combined weak lensing and X-ray survey with WFI@ESO/MPG-2.2 and XMM-Newton which eventually will cover 6 square degrees; observations of 4 square degrees have been finished. We observe fields for which deep publicly available XMM-Newton exposures exist. The almost perfectly matched FOVs of the XMM-Newton satellite and the WFI will allow us to look for X-ray counterparts for weak lensing detections and vice versa and study differences in the respective selection functions.

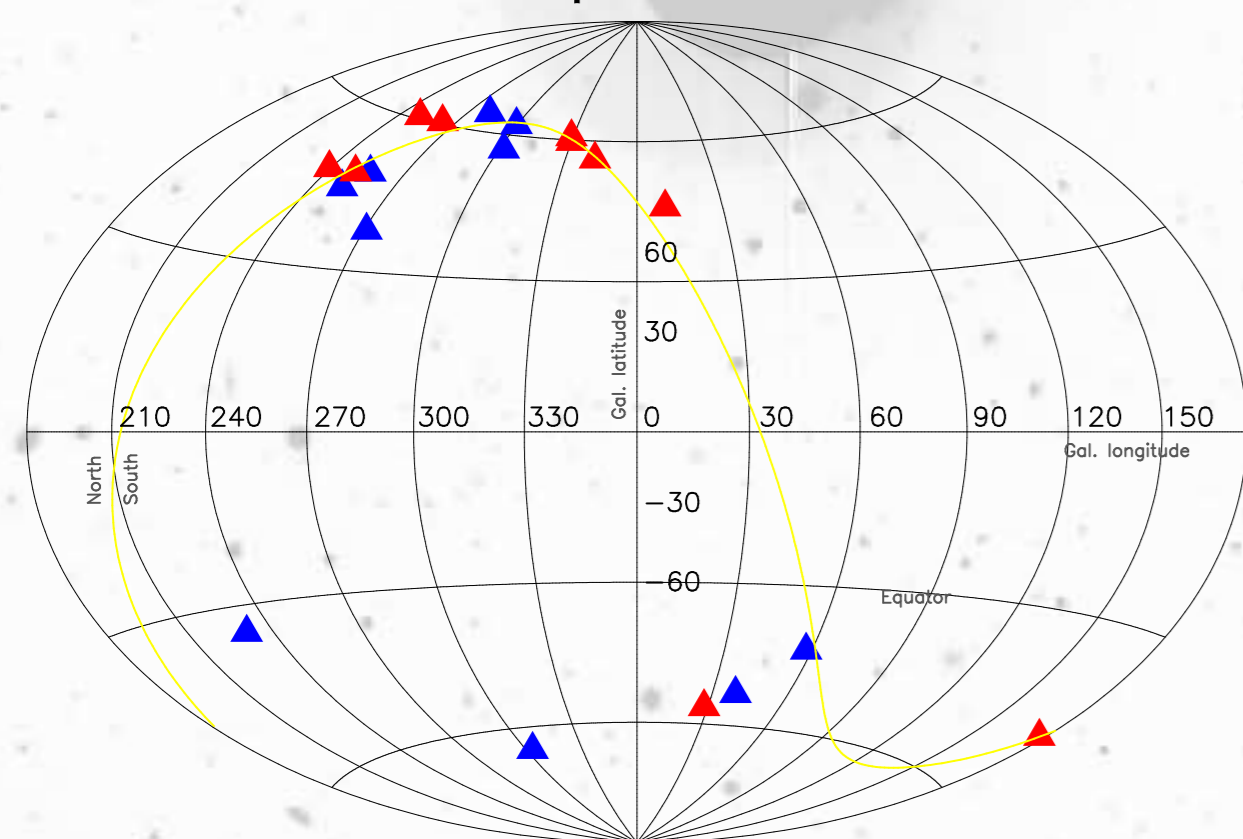


**Figure 1.** Field distribution of our survey in Galactic coordinates. Blue triangles mark fields from the ESO public survey observed in BVRI, red triangles are from our private survey observed in BR.

The survey is carried out in coordination with the XMM-Newton follow-up survey of the ESO Imaging Survey that contributes V- and I-band observations for some of the fields in which we supply the B- and R-band observations. R-band is the primary science band for the lensing analysis. Fig. 1 shows the distribution of our fields in Galactic coordinates. The reduced and calibrated data of the EIS public survey was recently released (Dietrich et al. 2005). The limiting magnitudes ( $5\sigma$ ,  $2''$ , AB system) are 25.0 mag for the BVR-band data and 24.5 mag for the I-band data.

## 3 Detection Method

Weak lensing shears the images of faint background galaxies (FBG). The shear pattern around massive foreground structures is illustrated in Fig. 2. The shear is oriented tangentially around massive structures. By locally averaging over the observed ellipticities of the FBG, the shear can be estimated.

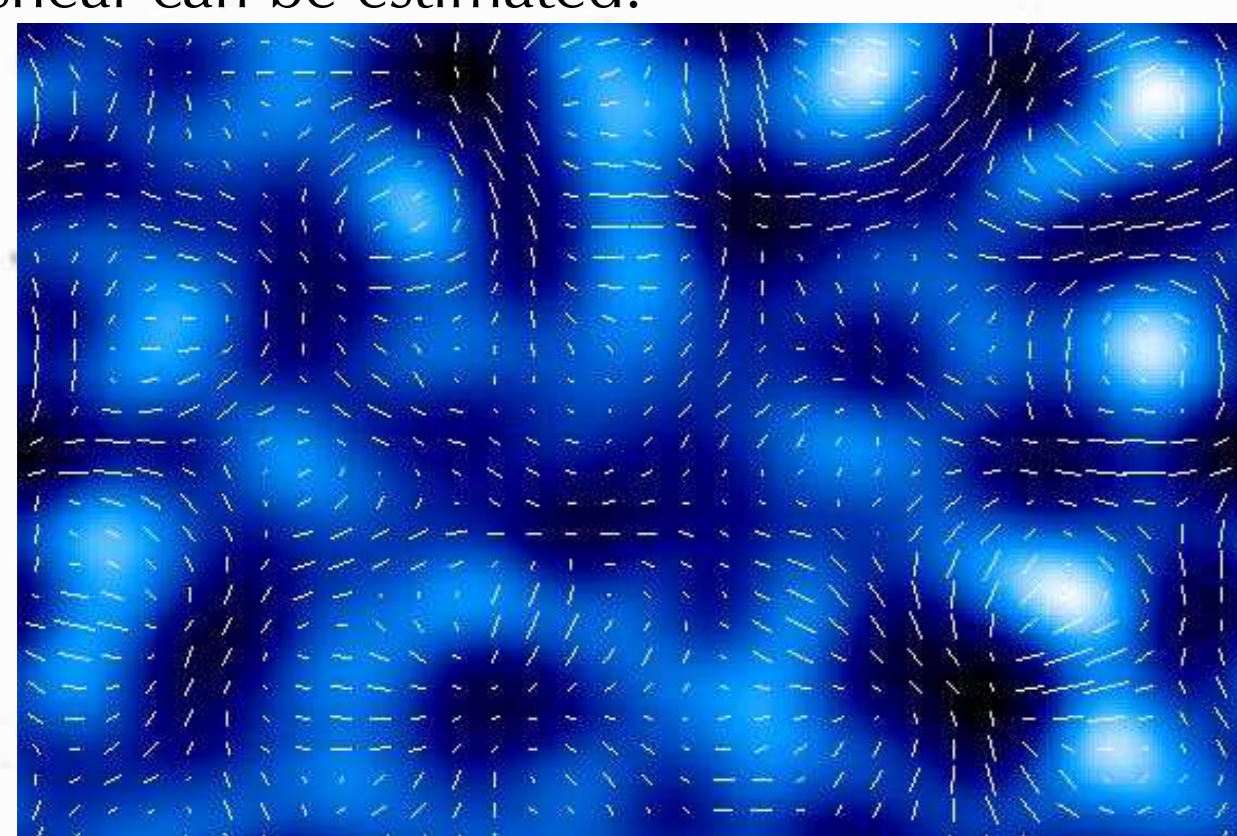


**Figure 2.** The color image in the background shows surface mass density, the sticks denote the shear pattern caused by this mass distribution.

The aperture mass statistics  $M_{\text{ap}}$  (Schneider 1996) is particularly suited for weak lensing searches for clusters of galaxies.  $M_{\text{ap}}$  is de-

defined as a weighted integral over the surface mass density  $\kappa$  in a (circular) aperture

$$M_{\text{ap}} = \int d^2\theta U(|\theta|) \kappa(\theta). \quad (1)$$

Because a sheet of constant surface mass density can be added without changing the shear, the weight function  $U(|\theta|)$  must have zero total weight:

$$\int d\theta \theta U(|\theta|) = 0. \quad (2)$$

It is possible to express  $M_{\text{ap}}$  in terms of the tangential shear  $\gamma_t$

$$M_{\text{ap}} = \int d^2\theta Q(|\theta|) \gamma_t(\theta) \quad (3)$$

with a weight function  $Q(|\theta|)$  that is related to  $U(|\theta|)$ .  $Q(|\theta|)$  can be optimized to follow the expected shear profile, in this case the aperture mass becomes a matched filter method for shear data.  $M_{\text{ap}}$  allows for an easy computation of the signal-to-noise ratio of a peak detection, either analytically

$$S/N = \frac{M_{\text{ap}}}{\sigma} = \sqrt{\frac{n}{\pi\sigma_\epsilon}} \frac{\int d^2\theta Q(|\theta|) \gamma_t(\theta)}{\int d^2\theta Q(|\theta|)}, \quad (4)$$

or by randomizing the orientation of the background galaxies and performing the computation of the  $M_{\text{ap}}$  statistics on the randomized catalogs to see how often the true signal exceeds the signal from the randomized catalog.

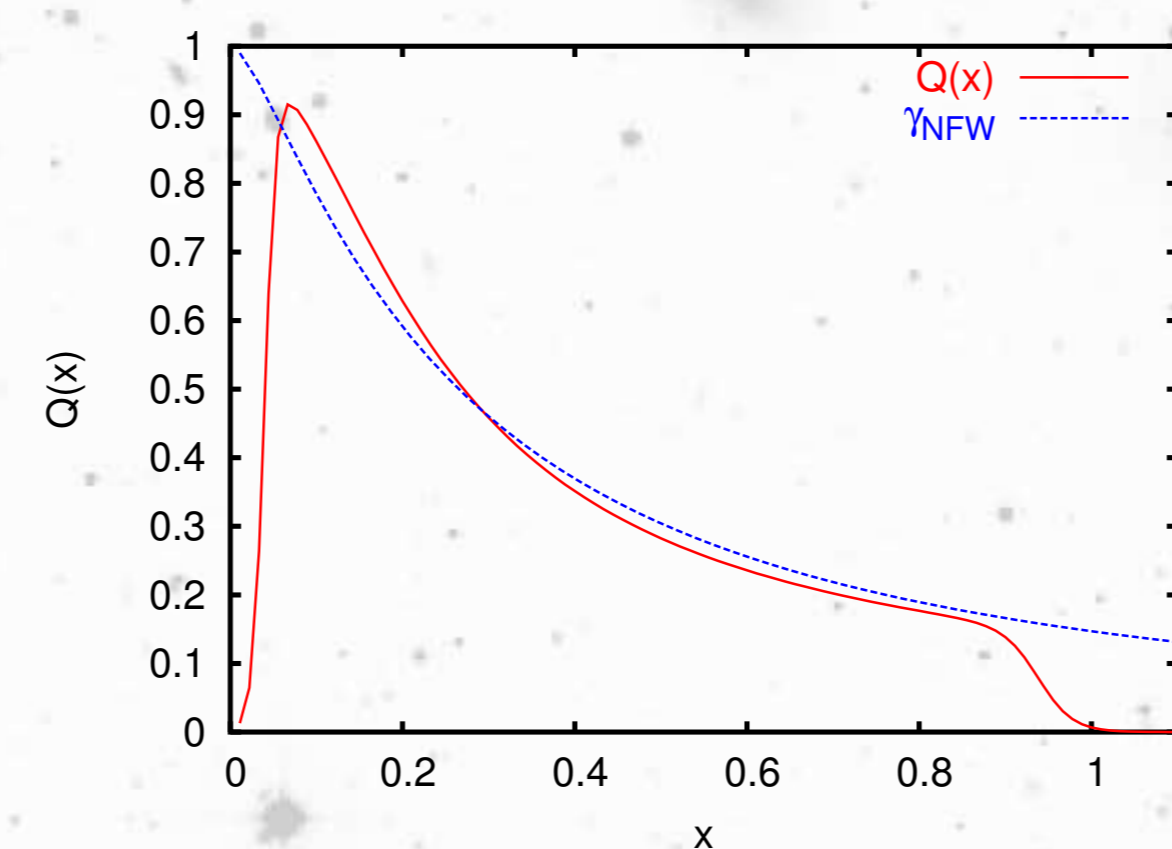


**Figure 3.** Comparison of the weight function  $Q(x)$  with the expected shear signal of an NFW halo.

As weight function  $Q$  we choose the function proposed by Schirmer (2004). This function closely follows the expected shear signal of an NFW halo with exponential cut-offs at large and small radii. These cut-offs avoid finite field effects and contamination by cluster dwarfs.

## 4 Weak Lensing Detections

The available data is fully reduced and a first sample of weak lensing detected cluster candidates has been defined. To search for cluster candidates we compute maps of the aperture mass in 15 different filter scales ranging from  $3\frac{1}{2}$  to  $19\frac{1}{8}$ . Every peak above a threshold of  $3\sigma$  in at least two filter scales is considered a cluster candidate and visually inspected. Figures 4 and 5 show two examples of such weak lensing selected cluster candidates.

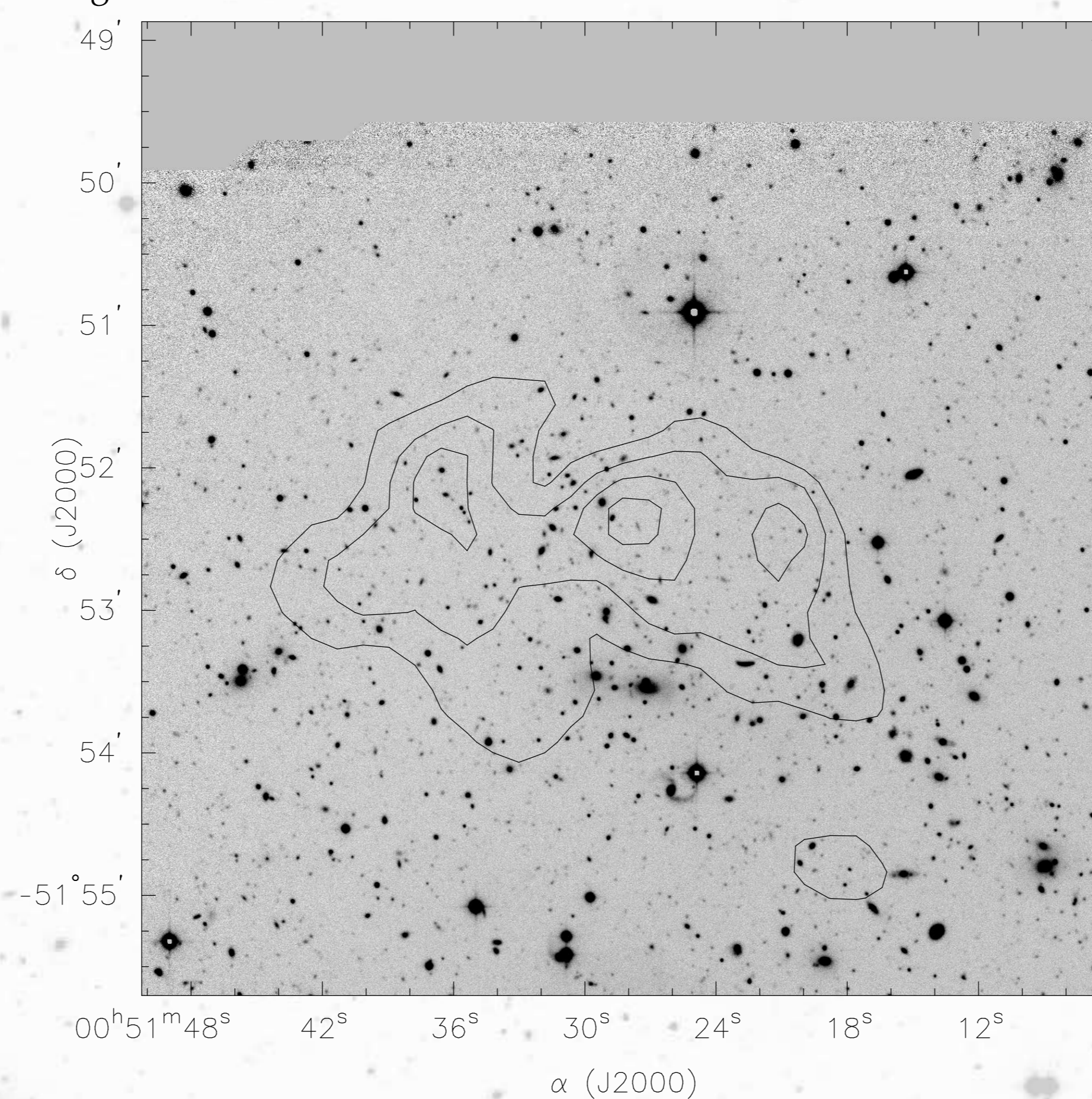


**Figure 4.** The weak lensing detected cluster candidate ClJ0551.5-5152. The image in the background is a  $6:8 \times 6:8$  cut-out from the WFI R-band image used for the lensing analysis. The contours are  $M_{\text{ap}}$  significance contours starting at  $1.5\sigma$  and increasing in steps of  $0.5\sigma$ . The peak significance is  $3.3\sigma$ .

In our analysis of 20 fields ( $\sim 4$  square degrees) we found 19 weak lensing selected satisfying our selection criteria cluster candidates with clear optical counterparts. 4 of these clusters were the primary target of the initial XMM-Newton observation. 10 XMM-Newton fields have been processed until now. We find 3 additional matches between X-ray and weak lensing selected clusters in these fields. The majority of all 19 cluster candidates is new and has not been previously reported as cluster or cluster candidate. We also find a number of shear selected peaks with uncertain optical counterparts, which require a more detailed optical analysis.

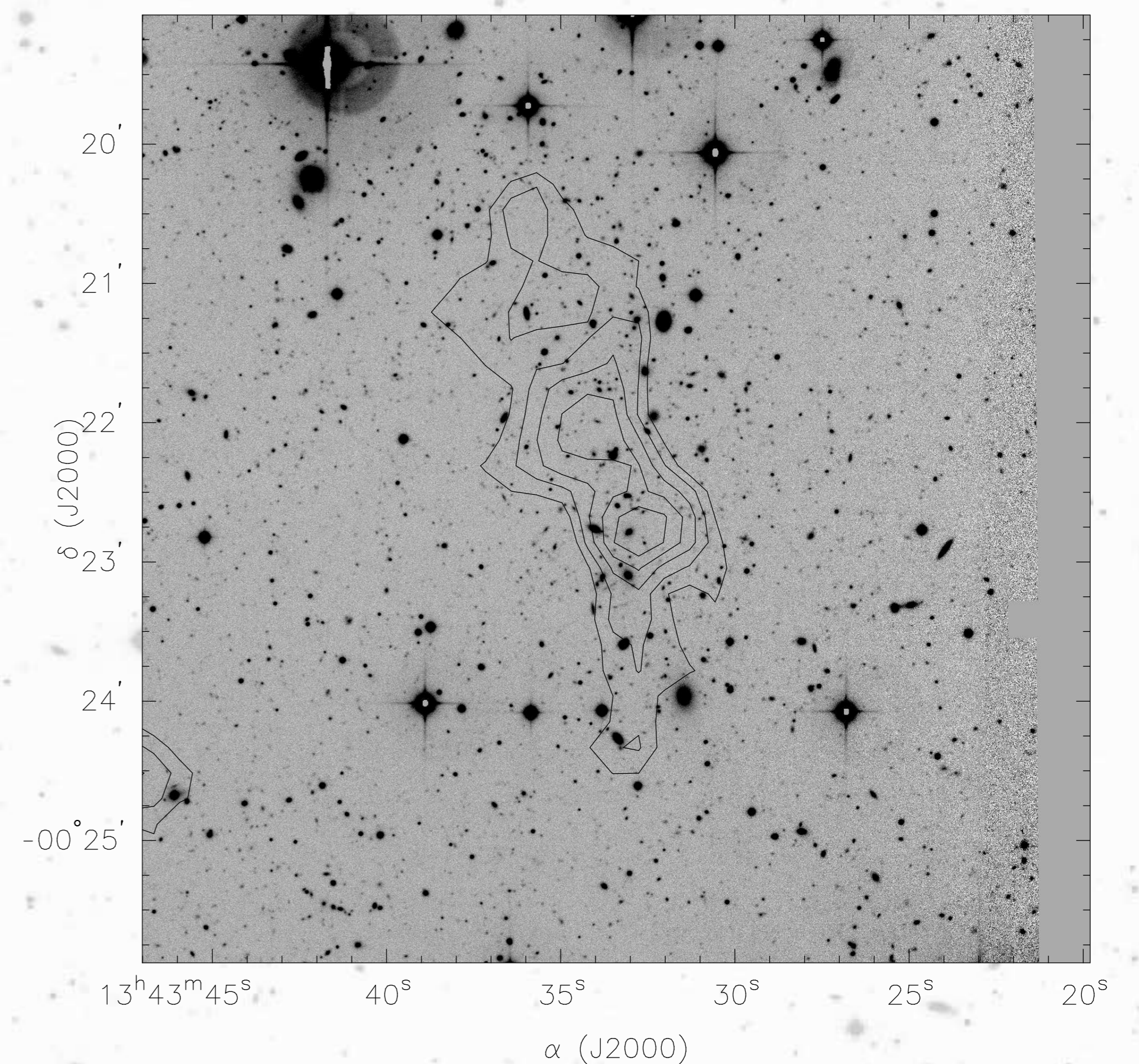


**Figure 5.** The shear-selected cluster candidate [LP96] Cl1341-0006. The cluster is detected with a significance of  $4\sigma$ . This object was previously identified as a cluster candidate by Lidman & Peterson (1996) using optical selection.

## 5 Outlook

Weak lensing, like optical cluster selection, is prone to projection effects along the line of sight. Eventually, all shear-selected cluster candidates will require spectroscopic confirmation. This will be of special importance for the weak lensing mass peaks with uncertain optical counterparts. We have proposed spectroscopic follow-up of a subsample for ESO P77, starting October 2006. A detailed comparison of weak lensing and X-ray properties, together with optical imaging and spectroscopy will reveal potential biases in either selection method. Hennawi & Spergel (2005) showed that weak lensing searches for clusters can be neither complete nor efficient, i.e., it is very difficult to derive cosmological parameters from simple cluster counts. To constrain cosmological models, we will compare the observed mass peak statistics with ray-tracing simulations through N-body simulations. Using a tomographic peak finder that uses photometric redshifts we will be able to increase completeness and efficiency on the public survey fields that have BVRI coverage.

## Acknowledgement

This work is based on observations taken at the ESO La Silla Observatory, Chile under Program Nos. 170.A-0789, 70.A-0529, 71.A-0110, 072.A-0061, 073.A-0050. This work has been supported by the German Ministry for Science and Education (BMBF) through DESY under the project 05AE2PDA/8, through DLR under the project 50 OX 0201, and by the Deutsche Forschungsgemeinschaft under the project SCHN 342/3-1.

## References

- Dietrich, J. P., Miralles, J.-M., Olsen, L. F., et al. 2005, A&A accepted, also astro-ph/0510223
- Eke, V. R., Cole, S., & Frenk, C. S. 1996, MNRAS, 282, 263
- Hennawi, J. F. & Spergel, D. N. 2005, ApJ, 624, 59
- Henry, J. P. 2004, ApJ, 609, 603
- Jenkins, A., Frenk, C. S., White, S. D. M., et al. 2001, MNRAS, 321, 372
- Lidman, C. E. & Peterson, B. A. 1996, AJ, 112, 2454
- Press, W. H. & Schechter, P. 1974, ApJ, 187, 425
- Schirmer, M. 2004, PhD thesis, Universität Bonn, Germany
- Schneider, P. 1996, MNRAS, 283, 837
- Vikhlinin, A., Voevodkin, A., Mullis, C. R., et al. 2003, ApJ, 590, 15
- Weinberg, N. N. & Kamionkowski, M. 2002, MNRAS, 337, 1269